Defence Life Science Journal, Vol. 5, No. 3, July 2020, pp. 163-172, DOI : 10.14429/dlsj.5.15254

Protein Profile of Human Lung Epithelial Cells (A549) Revealing Deviation in Cytoskeleton Proteins in Response to Zinc Oxide Nanoparticles Exposure

Avnika Singh Anand[#], Khushbu Jain[#], Rahul Ranjan[#], Dipti N. Prasad[#], Amitabh[#], Shashi Bala Singh[@], and Ekta Kohli[#,*]

[#]*DRDO-Defence Institute of Physiology and Allied Sciences, Delhi - 110 054, India*
[@]*National Institute of Pharmaceutical Education and Research, Hyderabad -500 037, India*
[*]*E-mail: ektakohli@dipas.drdo.in*

ABSTRACT

Zinc oxide nanoparticles (ZnO NPs) are widely used in biomedicine and scientific research because of their high dissolution property and bioavailability. On the contrary, this property also increases the intracellular reactivity, accessibility and cytotoxicity. These nano-bio interactions could induce undesirable changes in the proteome of the interacting cells, especially in the lung cells as these are the primary contact site. However, the potential effects of ZnO NPs exposure on proteome remain unclear. Proteomics data will substantiate the detailed mechanism of cellular interactions and modulatory effects of ZnO NPs on cells. Quantitative proteomic profiling was done using MALDI-TOF/TOF and MS/MS to identify differential protein expression on exposure to NPs among non exposed and exposed cells. Twenty-two proteins, with approximately 1.5 fold differential expression in cells exposed to ZnO NPs as compared to control cells were identified. Differentially expressed proteins were further classified using PANTHER software on the basis of functional gene ontology term: molecular function, biological process and cellular component. ToppGene suite was used to study protein-protein interaction and network was enriched with STRING. This study is a systematic analysis of protein modulation of the A549 cells exposed to ZnO NPs indicating alterations in the cytoskeleton.

Keywords: Proteomics; 2-D Electrophoresis; Zinc oxide nanoparticles; A549 cells

ABBREVIATION

BSA	Bovine serum albumin
PBS	Phosphate buffer saline
PFA	Paraformaldehyde
RT	Room Temperature
SEM	Standard error of mean
2-DE	Two-Dimensional Electrophoresis
CHAPS	3-[(3- Cholamidopropyl) dimethylammoniol]-1-propanesulfonate;
DTT	dithioreitol
TCA	Tricholoroacetic acid
SDS	Sodium dodecylsulfate
IEF	Isoelectric focusing

1. INTRODUCTION

Nanotechnology includes a material with the smallest unit of nanometre scale, ranging from 1-100 nm[1]. At the nanometer scale, many materials possess novel properties that are exploited in various applications[2]. With the increasing production of engineered nanoparticles (NPs), their release into the environment is drastically increased. It is important to study the adverse effects of the release of nanoparticles on the environment and human health[3] . The interaction of NPs with human tissues has not been fully elucidated. Nanoparticles have more surface area per unit mass, which make them very reactive in the cellular environment[4]. Humans can come in contact with NPs through inhalation; ingestion and absorption through skin[5,6]. Toxicity induced by engineered NPs remains debatable. Many questions remain unanswered concerning fate, communication and interactions of NPs with human cells.

Zinc oxide (ZnO) NPs with mystic properties are widely used in commercial products like textiles, plastic, paints, cosmetics, UV light blockers and medical supplies[7,8]. Toxicological studies on ZnO NPs have been conducted on various cell lines like human broncho-alveolar carcinoma derived cells, human lymphoblastoid cell line TK6, Chinese hamster ovary cells, human hepatocyte (L02) and human embryonic kidney (HEK293) cells; these studies primarily demonstrated oxidative stress, genotoxicity and homeostatic imbalance[9-12]. Due to high surface area and reactivity, NPs frequently interact with proteins and eventually these interactions can lead to conformational changes or loss of functionality of interacting or associated proteins. In the present report the differential proteomic response in A549 cells, on exposure to ZnO NPs was studied. The data indicated diverse patterns of cellular responses arising on exposure to the ZnO NPs and highlighted uncharacterised cellular phenomena. ZnO NPs have shown to induce cellular and morphological

Received : 23 November 2019, Revised : 19 May 2020
Accepted : 29 May 2020, Online published : 22 July 2020

modifications along with mitochondrial dysfunction and oxidative stress[13]. Through this study, we made an attempt to find the proteins regulating such mechanisms with a keen focus on protein related to the cytoskeleton. The outcome of this work will possibly be useful to determine the toxicity and biocompatibility of ZnO NPs, and enhance the understanding of nano-bio interactions.

2. METHODS

2.1 ZnO NPs Dispersion and Characterisation

The commercially purchased ZnO nanopowder (<50 nm) (Sigma Chemicals Co. Ltd.) were characterised on the basis of shape, size and stability by DLS and TEM. ZnO NPs dispersion was prepared in MilliQ water and cell culture medium, and ultra sonicated (ElmasonicS 30/H) for 10 min at 37 KHz. Hydrodynamic radii of the particles in dispersion was measured through dynamic light scattering with Malvern Zetasizer Nano-ZS (Malvern, U.S.A.). To determine the particle size and morphology, a drop of dispersion of NPs in MilliQ water was casted on 300 mesh carbon coated grid, air dried and visualised through TEM (MORGANI Instrument) at accelerating voltage of 200 KV.

2.2 Exposure of A549 Cells to ZnO NPs

The human lung carcinoma cell line (A549) was obtained from National Centre for Cell Sciences (Pune, India), tested for mycoplasma and endotoxin contamination and maintained at culture condition as given in Jain[13], *et al*. Lung carcinoma epithelial cells were cultured in Dulbecco's Modified Eagle's Medium high glucose supplemented with 10 % FBS, 100 unit mL^{-1} penicillin, 100 unit mL^{-1} streptomycin respectively. For proteomic studies, freshly prepared dispersion of 1 mg/ml ZnO NPs was diluted with cell culture media in required concentrations of 100 µg/ml, and added to A549 cells, and cells were cultured for 4 h at normal culturing conditions. Cells without ZnO NPs in culture media were considered as control.

2.3 Sample Preparation for Proteomics Analysis

In order to collect the cells for protein isolation, 0.1M PBS was added to cells that were scraped from the surface of the plate with a rubber policeman. The collected cells were centrifuged for 10 min at 300 g at 4 °C. Cell lysate was prepared by adding 200 µl of lysis buffer containing 40 mM Tris, 0.1 % NP 40, protease inhibitor cocktail and incubated for 30 min on ice. The lysed cells were centrifuged at 15000 g for 20 min and supernatant containing protein was collected[14,15].

2.4 Protein Precipitation with 10 % TCA

10 % TCA prepared in ice cold acetone was added to the protein supernatant in the ratio of 1:10 and incubated overnight at -20 °C. Pellet of precipitated protein was collected by centrifugation at 15,000 g for 10 min at 4 °C. The pellet was washed by incubating with 500 µl of 90 % ice cold acetone containing 20 mM DTT, for 10 min at -20 °C and centrifuged at 15000 g for 15 min at 4 °C. The pellet was washed repeatedly until clear white and then air dried. The pellet was dissolved in 100 µl of rehydration buffer (8 M urea, 2 % CHAPS, 0.2 % ampholyte, 50 mM DTT), quantified with Bradford assay and stored at -80 °C until further analysis[16].

2.5 Two-dimensional Gel Electrophoresis for Protein Separation

First dimensional gel separation was performed by rehydrating 7 cm, pH 4-7 IPG strip with 100 µg of protein in 125 µl of rehydration buffer (8 M urea, 2 % CHAPS, 0.2% ampholyte, 50 mM DTT, 0.001 % bromophenol blue) for 12 h. Isoelectric focussing was carried out at 100V, 30 min, rapid; 200-3500V, 1.5 h, gradient; 3500 V, 1-1.5 h, rapid and 500 V hold[17]. The strip was equilibrated with first equilibration buffer (50 mM Tris-HCL, pH 8.8, 6 M urea, 30 % glycerol (v/v), 2 % SDS (w/v), 1% DTT (w/v) and second equilibration buffer (DTT replaced with 2.5 % iodoacetamide) for 15 minutes. Second dimensional separation of proteins through electrophoresis was done on precasted gradient gels (4-20 %) at 100 V. The protein spots were visualised by silver staining and scanned image was analysed through Progenesis SameSpots and 2D gel image analysis software. Protein spots were analysed automatically and rechecked manually to ensure spots detection, matching and alignment. Detected protein spots with more than 1.5 fold difference and $p<0.05$ were selected for MALDI analysis.

2.6 In-gel Digestion and MALDI

In gel digestion was carried out to extract the peptide as per protocol described by Rubporn[18]. Briefly, proteins spots were excised from the gel and intensively washed with water. The excised spots were destained with 30 mM potassium ferric cyanide and 100 mM sodium thiosulphate for 30 min. The gel pieces were washed with water and 50 mM ammonium bicarboante/acetonitrile and incubated with 20 µl trypsin (1 µg/µL stock concentration, Promega Cooperation, Wisconsin, USA) at 37 °C for overnight followed by sonication for 10 min. The peptides were extracted with 0.1 % TCA and air dried in a speed vac. The peptide mixture was mixed with cyano-4 hydroxy-cinnamic acid matrix in a ratio of 1:1, spotted on MALDI plate and allowed to air dry. Mass standard were used to calibrate the instrument, peptide spectrum of the sample was further acquired through MALDI TOF/TOF (Ultraflex III, Bruker Daltonics, Bremen, Germany) at accelerating voltage of 25 KV in positive ion mode. The peptide data was exported and analysed through Biotools version 3.1, (Bruker Daltonics), Flex analysis 3.0 software and MASCOT search engine. The peptides were further identified using SWISS-PROT database with taxonomy as *Homo sapiens,* peptide mass tolerance of 100 ppm, maximum one missed cleavage site permitted and carbamidomethyl fixed modification as search parameters. The data obtained was further analysed for protein protein interaction using ToppGene suite. To understand the functional pathways related to the expressed proteins, the data set was analysed through PANTHER (Protein ANalysis THrough Evolutionary Relationship) software. The proteins were identified with UniProt accession dataset against the *Homo sapiens* reference dataset. The differentially

expressed proteins are classified into group of gene ontology, based on molecular function, biological process and cellular component. The differentially expressed proteins were also analysed for PANTHER pathway and protein class using PANTHER software.

2.7 Effect on cellular morphology on exposure to ZnO NPs

To study the change in cell morphology in reference to the proteomics data, expression of β tubulin was studied in A549 cells at 50 µg/ml and 100 µg/ml concentration of ZnO NPs. Approximatly, 1 x 10^5 /cm^2 cells were cultured on the coverslips and treated with 100 µg/ml and 50 µg/ml concentration of ZnO NPs individually for the period of 4 hours. The treated cells were further fixed with 3.7 % formaldehyde in 1X PBS for 5 min, washed thrice with 1X PBS and permeabilised with 0.1 % Triton X-100 in 1X PBS for 3 min. After washing thrice with 1X PBS, the cover slips were then blocked with 3 % bovine serum albumin in 1X PBS for 30 min at room temperature. Microtubulins were stained with mouse monoclonal anti β tubulin antibody at 1:100 dilution, subsequently the cells were incubated with FITC secondary antibody at 1:100 concentration. The images were acquired through a fluorescence microscope (Olympus BX51).

2.8 Statistical Analysis

All experiments were performed in triplicate with quantitative data represented as ± standard error of mean. Statistical analysis was done through Student's t-test using Graph Pad Prism software with statistically significant data with p-value < 0.05.Volcano plot was constructed to visualize differentiation protein expression using double filter criterion with negative log of the p-values on the y-axis (base 10), where the data points with low p-values i.e. considered being highly significant appears at the top of the plot. The values of log2 of the fold-change between the control and treated were plotted on the x axis. Fold change of ± 2 was considered to screen proteins with differential expression. Identical peptide quotients of the similar proteins were averaged and different peptides belonging to the same protein were averaged to determine the fold change.

3. RESULTS

3.1 Characterisation of ZnO NPs

Each particle behaves differently in biological media depending on its size and morphology. Distribution of these particles by intensity, volume in DMEM was measured by dynamic light scattering and transmission electron microscopy, showed no agglomerations[13,19]. ZnO NPs were spherically shaped with estimated size 23±3 nm. The hydrodynamic size of the particles was 110±2 nm with polydispersity index of 0.2 as determined through DLS as shown in Fig. 1.

3.2 Protein Profiling of Cells Exposed to ZnO NPs

A549 cells are human carcinoma alveolar basal epithelial cells that grow as monolayer adherent to the culture flask. Proteomic analysis was done on cell lysate of A549 cell treated with ZnO NPs at 100 µg/ml concentration for 4 h. The 2D gel electrophoresis was performed five times on control A549 cells and ZnO NPs exposed A549 cells. The representative protein pattern of A549 cells was shown in Fig. 2. An average of 185 and 163 spots was detected in control and ZnO NPs exposed cells, respectively. 22 differentially expressed protein spots were excised and digested with trypsin. The trypsinised peptides were further analysed by MALDI-TOF/TOF. A total of twenty two proteins from both cells were identified by MS/MS. Details of the differential protein expression in exposed and control cells were listed in Table 1. Eleven proteins were over expressed and eleven proteins were under expressed in ZnO exposed A549 cells by approximately 2-4 folds .The interaction map of differentially expressed proteins was generated through ToppGene suite as shown in Fig. 3. Differentially expressed proteins were broadly grouped into two categories; heat shock proteins and proteins related to the cytoskeleton.

3.3 Gene Ontology Analysis of Differentially Expressed Proteins

A cumulative result of the proteins with differential expression is illustrated in a volcano plot as shown in Fig. 4. The proteins were further identified on the basis of Gene ontology term GO biological process; immune system process, development process, cellular process, multicellular organismal process, metabolic process, cellular component

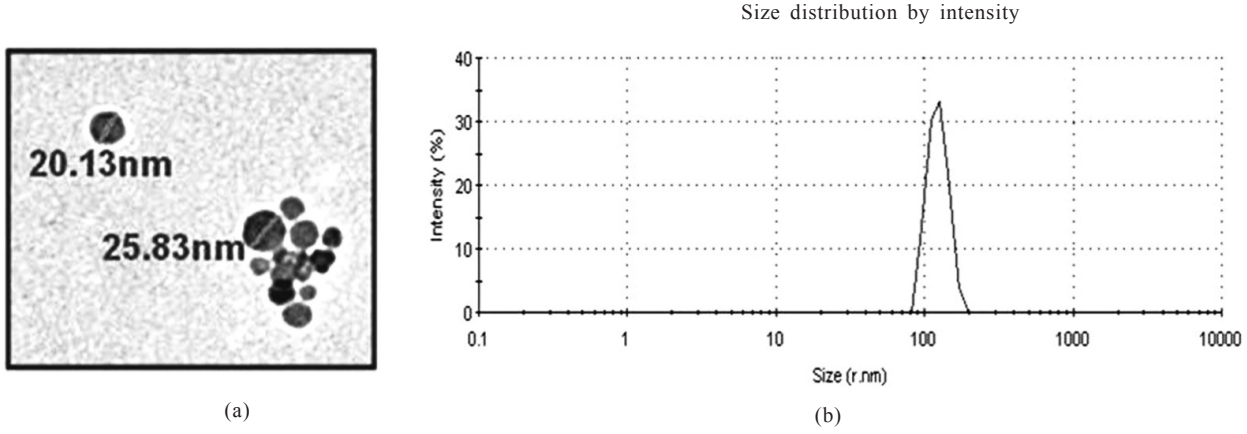

(a) (b)

Figure 1. (a) TEM image showing mono dispersed particles with an average size of 23 ± 3 nm and (b) Evaluation of hydrodynamic size and poly-dispersity index through dynamic light scattering.

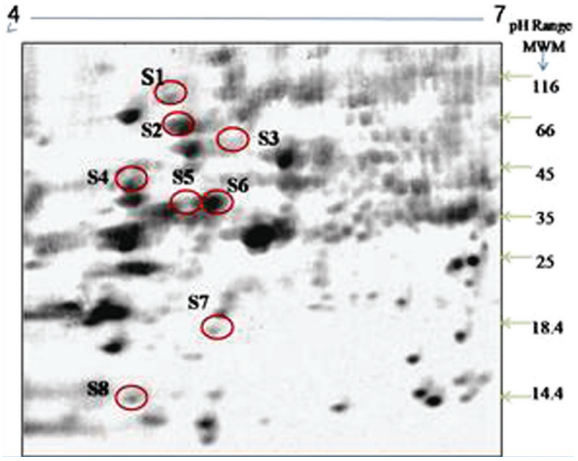

Figure 2. A representative 2-DE gel image of A549 cells exposed to ZnO-NPs (100 µg). Proteins (200 µg) were separated by IEF using pH 4-7, 7 cm IPG strips (Bio-rad) and 4-20% gradient gel. The gels were silver stained and analysed by Progenesis SameSpots 2-D gel image analysis software. Right indicate the migration of molecular mass standard (Thermo Scientific™ Pierce™ Unstained Protein MW Marker Catalog number:26610). Spot number represents differentially expressed proteins (± 2 fold, p<0.05) in ZnO exposed cells compared to control.

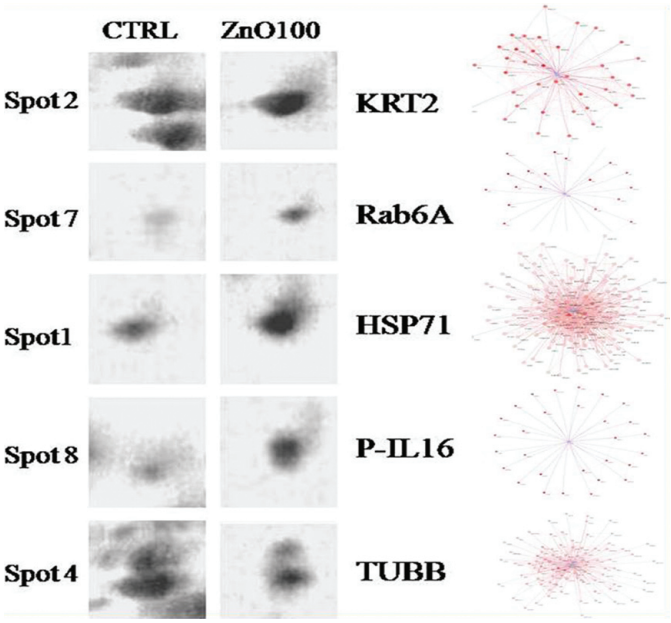

Figure 3. Zoom-in images of 2-D gel image of differentially expressed spots in control and ZnO-NPs exposed cells. Spots were identified by MS/MS. Interaction maps of differentially expressed proteins showing their interacting partners, using the ToppGene suite.

organisation and localisation GO molecular process; binding, structural molecule activity, catalytic activity and transporter activity; GO cellular component; macromolecular complex, cell part, organelle. PANTHER analysis was also done for protein class and cellular pathways, protein grouped into class of signalling molecule, transporter protein, cytoskeletal

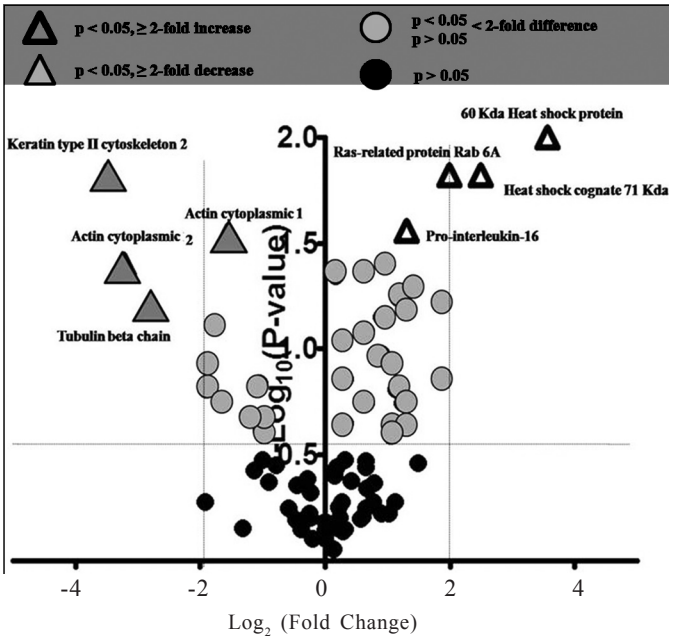

Figure 4. Volcano plot analysis showing differential protein expression in A549 cells treated with ZnO NPs. The relative level of protein expression after treatment is determined through statistical difference and fold change. The protein of interest are those away from the origin .The protein with increased expression are represented by open triangles while protein with decreased expression are represented by filled triangles. *X* axis shows the log2 of fold-change of the quotient ZnO-NPs exposed/control, whereas the *y* axis shows the − log10 of the calculated probability (p<0.05value), associated with Student's *t*-test.

protein, chaperone, enzyme modulator, structural protein, oxidoreductase and membrane traffic protein. Proteins regulating cellular pathways like cadherin signalling pathway, Interleukin signalling pathway, apoptosis signalling pathway, intergrin pathways, Alzheimer disease presenilin pathway, Huntington disease, inflammation mediated by chemokine and cytokine signalling pathways, wnt signalling pathway, Parkinson's disease, cytoskeleton regulation by Rho GTPase and Nicotine acetycholine receptor signalling pathways were altered on exposure with ZnO NPs as shown in Fig. 5.

To find relevant proteins among the multiple identifications obtained from proteomic analysis, we subjected the list of the 22 different proteins from Table 1 to bioinformatics analysis in the STRING database, which integrates interaction data from several bioinformatics sources and provides information about physical and functional properties, known and predicted interactions of genes and their products. Ten additional interacting proteins were added to provide a more comprehensive view of the interactions as shown in Fig. 6.

3.4 Effect on Cellular Morphology on Exposure to ZnO NPs

Contraction of cells was observed when stained with β-tubulin, indicating alteration of cytoskeleton structure on exposure to ZnO NPs as shown in Fig. 7. Control cells showed the normal microtubule network, whereas on exposure to ZnO

Table 1. Differential protein expression in A549 cells treated with ZnO NPs

Protein description	Accession No.	Mol. Wt.	Fold change	Mowse score	Gene function
3-hydroxyisobutyrate dehydrogenase, mitochondrial	P31937	35705	-1.5	38	Amino acid degradation pathway enzyme
6.8 kDa mitochondrial proteolipid	P56378	6658	-1.8	29	Component of an ATP synthase complex
60 kDa heat shock protein, mitochondrial	P10809	61016	**3.8**	64	Chaperonin, protein import, response to stress
Actin, cytoplasmic 1	P60709	42052	-1.8	84	Cell motility
Actin, cytoplasmic 2	P63261	42108	**-2.4**	88	Cell motility
Condensin complex subunit 3	Q9BPX3	115345	-1.5	28	Regulatory subunit of condensing, helps in cell division
FAD-dependent oxidoreductase domain-containing protein	Q96CU9	78085	-1.7	37	Oxidoreductase activity
Heat shock cognate 71 kDa protein	P11142	71082	**2.3**	81	Chaperon, regulation of transcription, response to stress
Keratin, type I cytoskeletal 10	P13645	59020	**-2.6**	64	Keratinocyte differentiation, calcium ion response
Keratin, type II cytoskeletal 2	P35908	65678	**-3.8**	62	Keratinocyte activation, terminal cornification
Keratin, type II cytoskeletal 7	P08729	51411	-1.8	60	Blocks interferon-dependent interphase and stimulates DNA synthesis
Metallothionein-2	P02795	7178	**2.2**	17	Metal metabolism and regulated by glucocorticoid
Pro-interleukin-16	Q14005	142976	1.2	96	Stimulates a migratory response in lymphocytes
Protein bicaudal D homolog 1	Q96G01	111252	1.7	42	Regulates coat complex coatomer protein I
Ras association domain-containing protein 2	P50749	37938	1.8	26	Potential tumour suppressor
Ras-related protein Rab-6A	P20340	23692	1.8	81	Protein transport
Thymosin beta-15A	P0CG34	5283	1.9	34	Organisation of the cytoskeleton
Tubulin beta chain	P10876	50095	**-2.9**	151	Microtubules
Vesicular integral-membrane protein VIP36	Q12907	40545	1.7	28	Intracellular lectin, involved in the transport and sorting of glycoproteins
Vimentin	P08670	53676	**-2.1**	44	Class-III intermediate filaments
Voltage-dependent anion-selective channel protein 2	P45880	32060	1.9	28	Forms a channel through the mitochondrial outer membrane
Voltage-gated potassium channel subunit beta-2	Q13303	41259	1.7	31	Accessory potassium channel protein

NPs, cells with damaged and disrupted morphology were observed. On exposure to ZnO NPs, shrinkage of cell were observed. In the control samples the microtubule network was well extended displaying normal cytoskeleton structure whereas in ZnO NPs treated cells this network was damaged and shrunken. Depolymerisation of the cytoskeleton and cell shrinkage are characteristic of apoptotic cell[20]. These observations postulate interaction of NPs with cytoskeleton related protein which also correlates with the results of proteomic analysis.

4. DISCUSSION

In the present study differential protein expression was obtained when A549 cells were exposed to ZnO NPs. We aimed to exploit the protein data to understand the cellular response of A549 cells to ZnO NPs. ZnO NPs are reported to induce oxidative stress, apoptosis, cell membrane disruption, lipid peroxidation and mitochondrial dysfunction [12,20]. Bioinformatics analysis of the data revealed that the altered proteins have diverse molecular functions, which suggests alteration of whole cellular proteome on ZnO-NPs exposure. The differential protein profile obtained as shown in Table 1 can be summarised into four categories; protein related to oxidative stress, mitochondria, folding and cytoskeleton. The heat shock proteins (Hsp) are molecular chaperones that mediate protein folding, transport and formation of protein structures that help the cells to survive in external stress. These include Hsp60, Hsp70, Hsp90, Hsp100 and Hsp110, each with a specific function. Hsp60 (chaperonin 60) and Hsp70 (cognate 11 proteins) were found to be significantly over expressed in the protein profile of A549 cells exposed with ZnO NPs. Over expression of these two proteins indicate towards the oxidative stress induced by the ZnO NPs. Hsp60 functions as a chaperone only in the mitochondria, which directs toward mitochondria as the target organelle effected by the ZnO NPs resulting in generation of free radicals. Hsp70

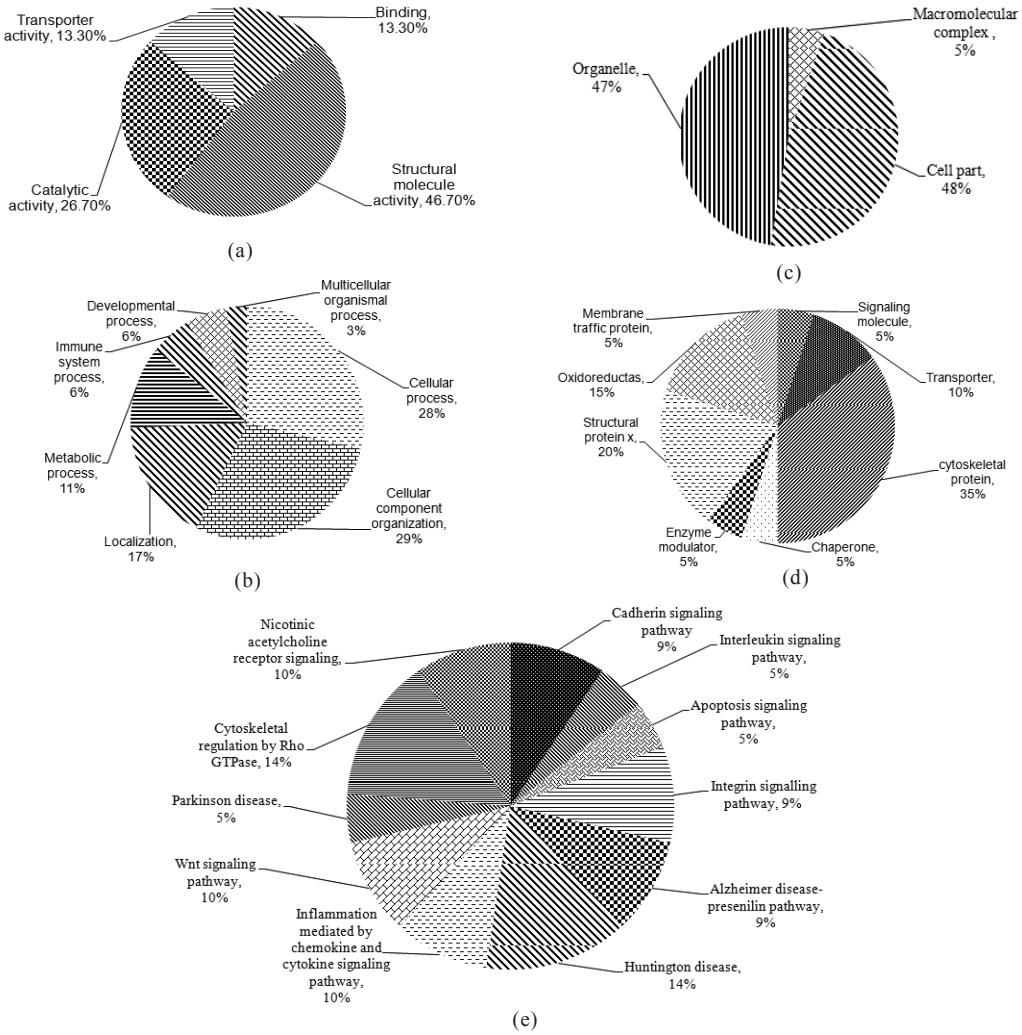

Figure 5. Categorisation of differentially expressed proteins based on gene ontology and pathways in ZnO-NPs exposed A549 cells compare to control, using PANTHER software (a) GO Biological process, (b) GO Molecular function, (c) GO Cellular component, (d) Protein class, (e) Pathway analysis.

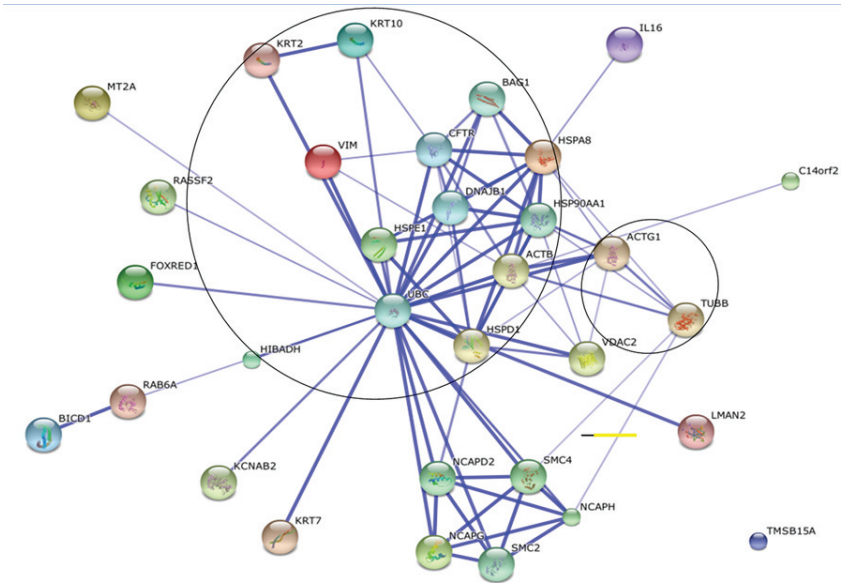

Figure 6. Bioinformatics analysis by Search Tool for the Retrieval of Interacting Genes/Proteins. The list of the identified protein was subjected to STRING analysis to reveal functional interactions between the deregulated proteins. Ten additional interacting proteins were added to provide a more comprehensive view of the interactions Each node represents a protein, and each edge represents an interaction.

functions in the cytoplasm and is frequently used as a marker in monitoring toxicity induced by metals[21], it is a promising marker in ZnO NPs toxicity profiling, a potential marker for tumor and targets lung cancer therapeutics[22]. Detoxification system of the cell has toxic effects on proteins. Increased expression of HSP70 indicates the preventive measure induced by the cell to protect various proteins from damage by improper folding.

Proteins related to stress response were found to be over expressed, combating against the induced oxidative stress; however most of the cytoskeleton related proteins like tubulin, actin and keratin were under expressed. β-tubulin heterodimer subunits are the building blocks of microtubules, expression of β-tubulin chain was three fold suppressed in cells exposed to ZnO NPs, indicating destabilisation of the microtubules. β-tubulin has microtubule stabilizing effects, under expression, result in shrinkage of cells as shown in Fig. 7, alteration in cell morphology and destabilisation of cell structure. Binding of the nanoparticles to tubulin could also bring permanent conformational alterations to the secondary structure, damage the microtubule polymerisation and weakening of mitochondria. With limited knowledge on NPs interaction with microtubules, the protein profile is indicative of cytoskeleton breakdown, cell division arrest and impaired cell motility.

The actin cytoskeleton is one of the major components of the cellular scaffold that is essential for maintaining cell shape and size[23]. Actin dynamics support a myriad of processes ranging from cell migration, division and morphogenesis to intracellular protein trafficking[24]. In a recent study, actin cytoskeleton signaling was differentially expressed when human lung cells were treated with CuNPs[25]. Gelatin nanoparticles were also reported to cause the F-actin cytoskeleton disruption and disorganisation[26]. Interestingly, in our experiments it was clearly observed through the proteome profile that expression levels of actin cytoplasmic 1 and actin cytoplasmic 2 was significantly reduced in cells treated with ZnO NPs. ZnO NPs are reported to cause irreparable damage to the actin structure and actin depolymerisation[27,28]. ZnO NPs cause damage to filamentous actin due to Ca^{2+} ion influx[29]. ZnO NPs mainly affect cytoskeleton protein actin and tubulin because of several binding sites of Zn^{2+} ions. Cytoskeleton protein actin and tubulin plays a vital role in maintaining zinc homeostasis. ZnO NPs treated HeLa cells showed formation of actin trails and abnormal actin accumulation[30].

GTP binding protein Ras functions in cytoskeleton organisation such as membrane ruffling, pinocytosis and formation of stress fibers[31,32]. Ras associated domain-containing protein 2, a potential tumor suppressor and Ras-related protein Rab-6A which is involved in protein transport was found to be over expressed. Vimentin is an important marker of tumor epithelial–mesenchymal cells[32] and is an important component of the cytoskeleton; it maintains the cell shape, integrity of cytoplasm, cell adhesion, and also involved in cell-cell interaction, cell mobility, proliferation, translation and transcription, apoptosis and cell signaling[33]. The proteome profile in our studies showed that expression level of Vimentin was reduced when A549 cells were treated with ZnO-NPs. The most important organelle targeted by ZnO-NPs is mitochondria; it is being reported that Vimentin influences cell movement through the mitochondria[34]. Mitochondria dysfunction could also be observed by differential expression of other proteins. AuNPs were reported to reverse the transition of epithelial-mesenchymal into cancer cells by down regulating vimentin[35]. This could also be the reason for reduced expression of vimentin when A549 are treated with ZnO-NPs, where tumor progression is impaired through a different pathway. Cytoskeleton plays a major role in regulating cell propagation and apoptosis; Keratin is one of the largest subgroups of intermediate filament proteins of cytoskeleton, with its function to protect the cell from stress[36]. Keratin, Type I and Keratin, Type II (Keratin type I cytoskeleton 10, Keratin type II cytoskeleton 2, Keratin cytoskeleton 7) were under expressed, these proteins are responsible for keratinocyte differentiation and activation[37]. NPs like CNTs, AgNPs and SiO_2 were reported to interact with cytoskeleton proteins[36,38,39].

In current study it was observed that ZnO NPs influence the expression of filamentous-Vimentin and various other filaments forming cytoskeleton protein like actin, tubulin and keratin, disturbing the cytoskeleton framework. Cytoskeleton proteins interact actively in the interactome, which suggests under-expression of these proteins affect cell's important functional pathways.

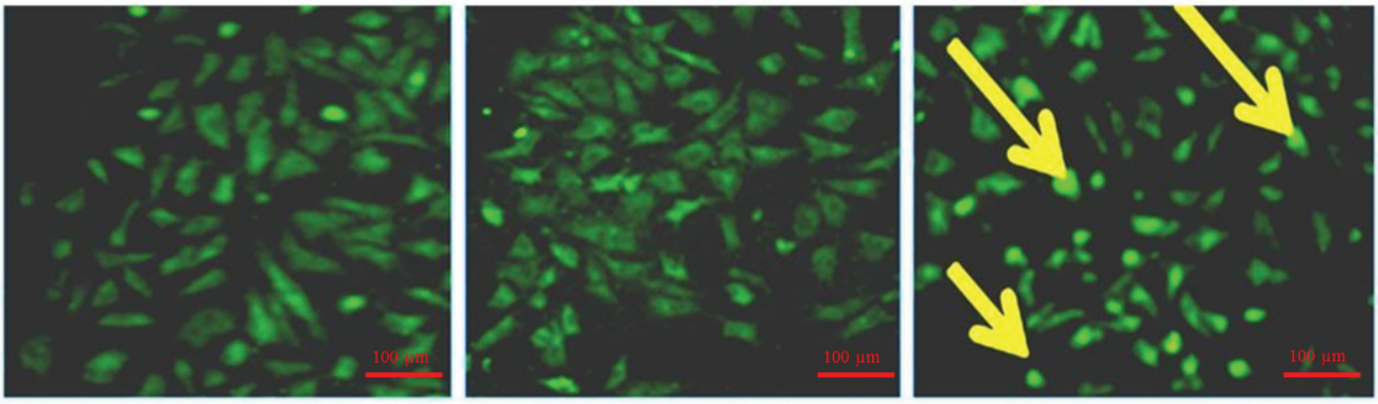

(a) (b) (c)

Figure 7. β-tubulin expression in A549 cells, (a) Normal cell morphology in untreated cells (b) Cells treated with 50 µg/ml ZnO NPs (c) Cells treated with 100 µg/ml ZnO NPs shows shrinkage and contraction.

5. CONCLUSION

In this paper we elucidated the interactions of ZnO NPs with cytoskeleton proteins. Heat shock proteins, cytoskeleton proteins like Keratin, Tubulin and Actin were differentially expressed in ZnO NPs exposed A549 cells. Toxicoproteomics highlighting protein interaction with NPs as the mechanism of toxicity was emphasised. Interactions of ZnO NPs resulted in shrinkage of cells due to disrupted cytoskeleton structure. A detailed understanding of mechanism of NM induced toxicity will facilitate the safer use of these materials in biomedicine, diagnostics and therapeutics.

Declarations of Interest

The authors report no declarations of interest.

REFERENCE

1. Silva, G.A. Neuroscience nanotechnology: Progress, opportunities and challenge. *Nature Rev. Neurosci.,* 2006, **7**(1), 65–74. doi: 10.1038/nrn1827
2. Huang, C.C.; Aronstam, R.S.; Chen, D. R. & Huang, Y.W. Oxidative stress, calcium homeostasis, and altered gene expression in human lung epithelial cells exposed to ZnO nanoparticles. *Toxicology In Vitro*, 2010, **24**(1), 45–55. doi: 10.1016/j.tiv.2009.09.007.
3. Oberdörster, G.; Oberdörster, E. & Oberdörster, J. Nanotoxicology: An emerging discipline evolving from studies of ultrafine particles. *Environmental Health Perspect*, 2005, **113**, 823–839. doi: 10.1289/ehp.7339
4. Wang, J.; Rahman, M.F.; Duhart, H.M.; Newport, G.D.; Patterson, T.A.; Murdock, R.C.; Hussain, S.M.; Schlager, J.J. & Ali, S.F. Expression changes of dopaminergic system-related genes in PC12 cells induced by manganese, silver, or copper nanoparticles. *Neurotoxicology*, 2009, **30**(6), 926–933. doi: 10.1016/j.neuro.2009.09.005.
5. Nohynek, G.J.; Lademann, J.; Ribaud, C. & Roberts, M.S. Grey goo on the skin? Nanotechnology, cosmetic and sunscreen safety. *Critical Rev. Toxicol.*, 2007, **37**(3), 251–277. doi: 10.1080/10408440601177780
6. Okoturo-Evans, O.; Dybowska, A.; Valsami-Jones, E.; Cupitt, J.; Gierula, M.; Boobis, A.R. & Edwards, R.J. Elucidation of toxicity pathways in lung epithelial cells induced by silicon dioxide nanoparticles. *PLoS One*, 2013, **8**(9), e72363. doi: 10.1371/journal.pone.0072363
7. Amara, S.; Slama, I.B.; Omri, K.; Ghoul, J.E.; El Mir, L.; Rhouma, K.B.; Abdelmelek, H. & Sakly, M. Effects of nanoparticle zinc oxide on emotional behavior and trace element homeostasis in rat brain. *Toxicology Industrial Health*, 2013, **31**(12), 1202-1209. doi: 10.1177/0748233713491802
8. Demir, E.; Akça, H.; Kaya, B.; Burgucu, D.; Tokgün, O.; Turna, F.; Aksakal, S.; Vales, G.; Creus, A. & Marcos, R. Zinc oxide nanoparticles: Genotoxicity, interactions with UV-light and cell-transforming potential. *J. Hazardous Materials*, 2009, **264**, 420–429. doi: 10.1016/j.jhazmat.2013.11.
9. Demir, E.; Creus, A. & Marcos, R. Genotoxicity and DNA Repair Processes of Zinc Oxide Nanoparticles. *Toxicol. Environmental Health*, 2014, **77**(21), 1292–1303. doi: 10.1080/15287394.2014.935540.
10. Huang, Y.-W.; Wu, C. & Aronstam, R.S. Toxicity of Transition Metal Oxide Nanoparticles: Recent Insights from in vitro studies. *Materials*, 2010, **3**(10), 4842–4859. doi: 10.3390/ma3104842
11. Pan, C.H.; Liu, W.T.; Bien, M.Y.; Lin, I.C.; Hsiao, T.C.; Ma, C.M.; Lai, C.H.; Chen, M.C.; Chuang, K.J. & Chuang, H.C. Effects of size and surface of zinc oxide and aluminum-doped zinc oxide nanoparticles on cell viability inferred by proteomic analyses. *Int. J. Nanomedicine*, 2014, **9**, 3631–3643. doi: 10.2147/IJN.S66651
12. Guan, R.; Kang, T.; Lu, F.; Zhang, Z.; Shen, H. & Liu, M. Cytotoxicity, oxidative stress, and genotoxicity in human hepatocyte and embryonic kidney cells exposed to ZnO nanoparticles. *Nanoscale Res. Lett.*, 2012, **7**(1), 602. doi: 10.1186/1556-276X-7-602.
13. Jain, K.; Kohli, E.; Prasad, D.; Kamal, K.; Hussain, S.M. & Singh, S.B. In Vitro Cytotoxicity Assessment of Metal Oxide Nanoparticles. *Nanomedicine Nanobiology*, 2014, **1**(1), 10–19. doi: 10.1166/nmb.2014.1003
14. Witzmann, F.A.; Clack, J.W.; Geiss, K.; Hussain, S.; Juhl, M.J.; Rice, C.M. & Wang, C. Proteomic evaluation of cell preparation methods in primary hepatocyte cell culture. *Electrophoresis*, 2002, **23**(14), 2223-2232. doi: 10.1002/1522-2683(200207)23:14%3C2223::AID-ELPS2223%3E3.0.CO;2-D
15. Bodzon-Kulakowska, A.; Bierczynska-Krzysik, A.; Dylag, T.; Drabik, A.; Suder, P.; Noga, M.; Jarzebinska, J. & Silberring, J. Methods for samples preparation in proteomic research. *J. Chromatography*, 2007, **849**(1-2), 1-31. doi: 10.1016/j.jchromb.2006.10.040
16. Fic, E.; Kedracka-Krok, S.; Jankowska, U.; Pirog, A. & Dziedzicka-Wasylewska, M. Comparison of protein precipitation methods for various rat brain structures prior to proteomic analysis. *Electrophoresis*, 2010, **31**(21), 3573–3579. doi: 10.1002/elps.201000197
17. Chhabra, V.; Anand, A.S.; Baidya, A.K.; Malik, S.M.; Kohli, E. & Reddy, M.P.K. Hypobaric hypoxia induced renal damage is mediated by altering redox pathway. *PloS one*, 2018, **13**(7). doi: 10.1371/journal.pone.0195701
18. Rubporn, A.; Srisomsap, C.; Subhasitanont, P.; Chokchaichamnankit, D.; Chiablaem, K.; Svasti, J. & Sangvanich, P. Comparative proteomic analysis of lung cancer cell line and lung fibroblast cell line. *Cancer Genomics Proteomics*, 2009, **6**(4), 229–237.
19. Patel, P.; Kansara, K.; Senapati, V.A.; Shanker, R.; Dhawan, A. & Kumar, A. Cell cycle dependent cellular uptake of zinc oxide nanoparticles in human epidermal

cells. *Mutagenesis*, 2016, **31**(4), 481-490.
doi: 10.1093/mutage/gew014

20. Akhtar, M.J.; Ahamed, M.; Kumar, S.; Khan, M.M.; Ahmad, J. & Alrokayan, S.A. Zinc oxide nanoparticles selectively induce apoptosis in human cancer cells through reactive oxygen species. *Int. J. Nanomed.*, 2012, **7**, 845.
doi: 10.2147%2FIJN.S29129
21. Doğanlar, Z.B.; Doğanlar, O. & Tabakçioğlu, K. Genotoxic effects of heavy metal mixture in Drosophila melanogaster: Expressions of heat shock proteins, RAPD profiles and mitochondrial DNA sequence. *Water, Air Soil Pollution*, 2014, **225**(9).
doi: 10.1007/s11270-014-2104-9
22. Seiwert, T.Y.; Tretiakova, M.; Ma, P.C.; Khaleque, M.A.; Husain, A.N.; Ladanyi, A.; Chen, L.B.; Bharti, A. & Salgia, R. Heat shock protein (HSP) overexpression in lung cancer and potential as a therapeutic target. *Cancer Research*, 2005, **65**, 559–560.
23. Hotulainen, P. & Hoogenraad, C. C. Actin in dendritic spines: connecting dynamics to function. *J. Cell Biology*, 2010, **189**(4), 619-629.
doi: 10.1083/jcb.201003008
24. Cingolani, L.A. & Goda, Y. Actin in action: the interplay between the actin cytoskeleton and synaptic efficacy. *Nature Rev. Neurosci.*, 2008, **9(**5), 344–356.
doi: 10.1038/nrn2373.
25. Edelmann, M.J.; Shack, L.A.; Naske, C.D.; Walters, K.B. & Nanduri, B. SILAC-based quantitative proteomic analysis of human lung cell response to copper oxide nanoparticles. *PLoS One*, 2014, **9**(12), e114390.
doi: 10.1371/journal.pone
26. Gupta, A.K.; Gupta, M.; Yarwood, S.J. & Curtis, A.S.G. Effect of cellular uptake of gelatin nanoparticles on adhesion, morphology and cytoskeleton organisation of human fibroblasts. *J. Controlled Release*, 2004, **95**(2), 197–207.
doi: 10.1016/j.jconrel.2003.11.006
27. Liu, J.; Kang, Y.; Yin, S.; Song, B.; Wei, L.; Chen, L. & Shao, L. Zinc oxide nanoparticles induce toxic responses in human neuroblastoma SHSY5Y cells in a size-dependent manner. *Int. J. Nanomed.*, 2017, **12**, 8085.
doi: 10.2147%2FIJN.S149070
28. Pati, R.; Das, I.; Mehta, R.K.; Sahu, R. & Sonawane, A. Zinc-oxide nanoparticles exhibit genotoxic, clastogenic, cytotoxic and actin polymerization effects by inducing oxidative stress responses in macrophages and adult mice. *Toxicological Sciences*, 2016, **150**(2), 454-472.
doi: 10.1093/toxsci/kfw010
29. García-Hevia, L.; Valiente, R.; Martín-Rodríguez, R.; Renero-Lecuna, C.; González, J.; Rodríguez-Fernández, L.; Aguado, F.; Villegas, J.C. & Fanarraga, M.L. Nano-ZnO leads to tubulin macrotube assembly and actin bundling, triggering cytoskeletal catastrophe and cell necrosis. *Nanoscale*, 2016, **8**(21), 10963-10973.
doi: 10.1039/C6NR00391E
30. Bar-Sagi, D. & Feramisco, J.R. Induction of membrane ruffling and fluid-phase pinocytosis in quiescent fibroblasts by ras proteins. *Science*, 1986, **233**(4768), 1061–1068.
doi: 10.1126/science.3090687
31. Ridley, A.J. & Hall, A. The small GTP-binding protein rho regulates the assembly of focal adhesions and actin stress fibers in response to growth factors. *Cell*, 1992, **70**(3), 389–399.
doi: 10.1159/000101320
32. Kokkinos, M.I.; Wafai, R.; Wong, M.K.; Newgreen, D.F.; Thompson, E.W.; Waltham, M. Vimentin & epithelial-mesenchymal transition in human breast cancer--observations in vitro and in vivo. *Cells Tissues Organs*, 2007, **185**(1-3), 191–203.
doi: 10.1159/000101320
33. Ivaska, J.; Pallari, H.M.; Nevo, J. & Eriksson, J.E. Novel functions of vimentin in cell adhesion, migration, and signaling. *Experimental Cell Research*, 2007, **313**(10), 2050–2062.
doi: 10.1016/j.yexcr.2007.03.040
34. Nekrasova, O.E.; Mendez, M.G.; Chernoivanenko, I.S.; Tyurin-Kuzmin, P.A.; Kuczmarski, E.R.; Gelfand, V.I.; Goldman, R.D. & Minin, A.A. Vimentin intermediate filaments modulate the motility of mitochondria. *Mol. Biol. Cell*, 2011, **22**(13), 2282–2289.
doi: 10.1091/mbc.E10-09-0766
35. Arvizo, R.R.; Saha, S.; Wang, E.; Robertson, J.D.; Bhattacharya, R. & Mukherjee, P. Inhibition of tumor growth and metastasis by a self-therapeutic nanoparticle. *In* Proceedings of the National Academy of Sciences, 2013, **110**(17), 6700–6705.
doi: 10.1073/pnas.1214547110
36. Yang, X.; Liu, J.; He, H.; Zhou, L.; Gong, C.; Wang, X.; Yang, L.; Yuan, J.; Huang, H.; He, L.; Zhang, B. & Zhuang, Z. SiO2 nanoparticles induce cytotoxicity and protein expression alteration in HaCaT cells. *Particle Fibre Toxicol.*, 2010, **7**(1), 1.
doi: 10.1186/1743-8977-7-1
37. Zhang, L.J. Keratins in Skin Epidermal Development and Diseases. *IntechOpen*, 2018.
doi: 10.5772/intechopen.79050
38. Holt, B.D.; Short, P.A.; Rape, A.D.; Wang, Y.L.; Islam, M.F. & Dahl, K.N. Carbon nanotubes reorganize actin structures in cells and ex vivo. *ACS Nano*, 2010, **4**(8), 4872-4878.
doi: 10.1021/nn101151x
39. Xu, F.; Piett, C.; Farkas, S.; Qazzaz, M. & Syed, N.I. Silver nanoparticles (AgNPs) cause degeneration of cytoskeleton and disrupt synaptic machinery of cultured cortical neurons. *Molecular Brain*, 2013, **6**(1), 29.
doi:10.1186/1756-6606-6-29

ACKNOWLEDGEMENTS

We thankful to Department of Science and Technology, New Delhi for providing fellowship for this study. Authors thankful to Council of Scientific and Industrial Research for providing fellowship for this study. Authors are also thankful to All India Institute of Medical Sciences, New Delhi for TEM analysis in the current study.

CONTRIBUTORS

Ms Avnika Singh Anand is currently working as DST INSPIRE research fellow at DRDO-Defence Institute of Physiology and Allied Sciences, Delhi. She is working on toxicity of metal oxide nanoparticles.
In the current study, She has worked in designing this work and carried out experiments.

Dr Khusbhu Jain has received her PhD from Bharathiar University. She worked as CSIR research fellow at DRDO-Defence Institute of Physiology and Allied Sciences, Delhi.
In the current study, She has contributed in experiment design and carried out various experiments.

Mr Rahul Ranjan iis currently working as Research Fellow DRDO-Defence Institute of Physiology and Allied Sciences, Delhi.
In the current study, he has contributed in analysis and interpretation of bioinformatics data.

Dr Dipti Prasad is Scientist 'F' and Head of Neurobiology Department, Defence Institute of Physiology and Allied Sciences, DRDO.
In the current study, she has contributed in drafting and reviewing of the manuscript

Mr Amitabh is Technical Officer at Department of Neurobiology, DRDO-Defence Institute of Physiology and Allied Sciences, Delhi.
In the current study, he has contributed in reviewing of the manuscript.

Dr Ekta Kohli is Scientist 'E' at DRDO-Defence Institute of Physiology and Allied Sciences, DRDO. Her major research area is Nanotechnology and Toxicology. She has publications in International Journals, chapters, and patent to her credit.
In the current study, She has contributed in thorough experimental design, execution, analysis, interpretation of results and writing of the manuscripts.

Dr Shashi Bala Singh is superannuated as Director General, Life Sciences, DRDO. She has immensely contributed to the understanding of high altitude physiology and pioneered the development of nutraceuticals and prophylactics for several high altitude maladies that include hypophagia and cognitive impairment.
In the current study, she was involved in drafting and reviewing of the manuscript.